



# Evaluating seismic risk by MCDM and machine learning for the eastern coast of India

Abhishek K. Rai · Sukanta Malakar ·  
Susmita Goswami

Received: 17 October 2023 / Accepted: 5 April 2024 / Published online: 25 April 2024  
© The Author(s), under exclusive licence to Springer Nature Switzerland AG 2024

**Abstract** Natural disasters such as earthquakes endanger human lives and infrastructure, particularly in urban areas. With the advancements in science and technology in understanding natural hazards, recent studies have attempted to mitigate them by mapping the risks using geospatial technology. In this paper, we attempt to integrate the multi-criteria decision-making (MCDM) models, namely the Analytical Hierarchy Process (AHP) and the Criteria Importance Through Inter-criteria Correlation (CRITIC), besides using the artificial neural network (ANN) to assess the seismic risk in the eastern coast of India. The AHP-CRITIC technique is used to evaluate the earthquake coping capacity and vulnerability and has been further used to generate a training base for earthquake probability mapping by ANN. The earthquake probability and spatial intensity information are used to develop the hazard map. Following that, integrating vulnerability, hazard and coping capacity spatial information assessed earthquake risk. Our results indicate that approximately 5% of the study area is at high risk, whilst more than 11% of the population is at high risk due to seismic induced hazards. The area under the curve of the receiver operating characteristic curve is 0.85, which indicates reliable results.

The results of this study may help various agencies involved in planning, development and disaster mitigation to develop seismic hazard mitigation methods by better understanding their impacts on the eastern coastal region of India.

**Keywords** Earthquake vulnerability · Hazard · Risk · East coast of India · MCDM · ANN

## Introduction

Earthquakes and their secondary effects are amongst the most destructive natural hazards, with adverse long-term impacts on societies (Singh et al., 2012). According to the Centre for Research on the Epidemiology of Disasters (CRED, 2015), after flooding and landslides, earthquakes were the third most common natural disaster from 1994 to 2013, causing \$787 billion in damage. It is also noted that earthquakes and related disasters have been the deadliest natural hazards over the last two decades, accounting for 55% of all fatalities (Alexander, 2018). According to the researchers, the exact time, magnitude and location of occurrence of earthquakes are still unpredictable (Malakar et al., 2023; Rai et al., 2023). Hence, it is essential to have efficient strategies to detect potential earthquake risk zones through geospatial techniques.

Geomorphologically and tectonically, the Indian east coast is segmented into the Cauvery, Palar, Krishna-Godavari, Mahanadi and Bengal Basins.

A. K. Rai (✉) · S. Malakar · S. Goswami  
Centre for Ocean, River, Atmosphere and Land Sciences (CORAL), Indian Institute of Technology Kharagpur, Kharagpur 721302, West Bengal, India  
e-mail: abhishek@coral.iitkgp.ac.in

This segmentation indicates the East Coast subcrustal deformation (Radhakrishna, 1989). Though the east coast was deemed a relatively stable continental margin, active faults are now documented along the coast and offshore. In the Indian peninsula, instrument-recorded global seismic events noted few earthquake events. Banerjee et al. (2001) concluded that the Indian peninsular shield was practically aseismic until the 1960s, making it essential to map the areas affected by slope failure, active faults and changes in seabed morpho-bathymetric patterns. Seismicity evidence along the coast and adjoining offshore must be investigated. The moderate-magnitude intraplate earthquake in Tamil Nadu (Mw 5.5, 2001) has created enough interests in understanding the rejuvenation of seismic activity along some of the zones of weakness. Neotectonic earthquakes may also cause damage to infrastructure (Rai & Nayak, 2021). Hence, a comprehensive earthquake study is required, and researchers should focus on using recent computing techniques like machine learning.

Over the years, several researchers have attempted to study earthquake-associated hazards using machine learning techniques. Alizadeh et al. (2018) tried to incorporate the analytical network process (ANP) and artificial neural network (ANN) to assess the earthquake vulnerability of Tabriz City, Iran. Jena et al. (2019) integrated the information of the analytical hierarchy process (AHP) with the ANN to assess the seismic risk for Banda Aceh, Indonesia, whereas Jena and Pradhan (2020) used ANN-cross validation for the probability mapping and AHP-Technique for Order of Preference by Similarity to Ideal Solution (TOPSIS) to map the vulnerability. This model to enhanced the accuracy of earthquake risk mapping in Banda Aceh, Indonesia. Yariyan et al. (2020) used a fuzzy AHP-ANN model to assess seismic risk spatially in Sanandaj, Iran; however, Yariyan et al. (2021) estimated seismic vulnerability in Sanandaj using different hybrid ANN models, and later they compared the developed results. Malakar et al. (2022) integrated AHP and Entropy with ANN to map the earthquake risk in the Himalayas. Moreover, machine-learning techniques for landslide and flood susceptibility mapping, potential groundwater mapping and other environmental applications have been successfully implemented.

In India, integration of ANN and geospatial techniques has been used in a few studies; however, the

available literature search show limited studies that have evaluated the seismic risk on the east coast of India, taking into account vulnerability and coping capacity. Jena et al. (2020) used the recurrent neural network to assess earthquake probability in the Odisha region, India, whilst for estimating the seismic vulnerability, Jena et al. (2021a) combined AHP with a probabilistic neural network. These studies reported moderate to very low earthquake probability in the coastal part of Odisha. Malakar and Rai (2023) used integrated multi-criteria decision-making (MCDM) models to predict seismic vulnerability in West Bengal and found that the Sundarban region on the east coast of India falls under a very low to moderate seismic vulnerability zone. Mukhopadhyay et al. (2016) and Karuppusamy et al. (2021) developed a multi-hazard-risk map in the Balasore coast, Odisha and coastal plains of Tamil Nadu, including coastal erosion, tropical cyclones, storm surges, coastal flooding, sea level rise, tsunamis and earthquakes using multi-criteria analysis. The results demonstrate that the eastern coastal region has not suffered any major earthquake in the past; however, peak ground acceleration and earthquake data show that the Balasore coast and the northern Coromandel Coast in Tamilnadu are susceptible to moderate destructive threats (Zone III). Hence, we attempted to conduct a comprehensive earthquake risk study for the east coast plain of India for the first time to help develop mitigation strategies. Usually, researchers who have done risk assessments using ANN usually restrict themselves to a small area. The primary reason is the lack of availability of datasets. Accumulating large-scale datasets is quite challenging, and some countries are banned from the availability of datasets. So, the researchers are focused on small areas rather than large-scale scenarios. It is also found from the literature review that the researchers who have integrated the MCDM model and ANN to estimate the seismic hazard have used a single MCDM model, primarily AHP, except Jena and Pradhan (2020) and Malakar et al. (2022). The AHP weights are obtained from previously available literature and expert knowledge. Experts typically ignore data information when calculating weights with AHP, leading to uncertainty (Bhattacharya et al., 2010); however, integrated MCDM models might deal with this problem (Malakar & Rai, 2022a, 2022b). All these limitations lead to the objectives of our study.

The main objectives of our study are: a) to propose a novel methodology for estimating the earthquake risk for the eastern coastal plain of India through integrated subjective AHP and objective CRITIC multi-criteria decision-making models with ANN and spatial information; b) to obtain freely available datasets that have a direct and indirect influence on earthquake risk estimation; and c) to examine the sensitivity and performance of the model and validate the developed result with high impact published literature. In the following sections we present the methodology and data sources in detail.

## Study area

Indian landmass includes nearly ~7500 km long coastline with dynamic and varied coastland landforms, including sediment, rock and coral-based landforms (Mukhopadhyay & Karisiddaiah, 2014). This diverse and dynamic coastland has resulted from varied tectonic activity affecting lithology, besides monsoonal climate and sea-level fluctuations.

The east coast of India stretches from north to south across the Indian states of West Bengal, Orissa, Andhra Pradesh and Tamil Nadu, having an area of about 387,844 sq. km with an inhabitant of more than 200 million (Fig. 1). The Ganga–Brahmaputra, Mahanadi, Krishna, Kaveri and Godavari are the major rivers which drain the eastern coastline area, forming major offshore sedimentary basins with sediment thicknesses of up to 5 km (Murthy et al., 2012). The east continental margin existed between 140 and 120 million years ago when India separated from East Antarctica and drifted at the ‘bight’ where the Krishna-Godavari Basin is presently located (Mukhopadhyay & Karisiddaiah, 2014). Murthy et al. (2012) concluded that India possibly broke apart from East Antarctica in two stages, resulting in the NE-SW oriented Krishna-Godavari rift and N-S oriented Kaveri shear segments.

Since the last century, this region has witnessed moderate seismicity, indicating the Precambrian faults’ reactivation or tectonic activity (Murthy et al., 2006). The seismological section identified a series of faults cutting through Jurassic sediments from Paradip to the west of the Ganga Delta (GSI, 2005). Precambrian basement has been picked up from the coastline to 75 km seaward in Mahanadi

offshore, 3 km beneath the coast and 8.5 km offshore, and faulted in various areas (GSI, 2002). The Geological Survey of India (GSI) conducted shallow seismic surveys and observed fault signatures along the east coast’s offshore domains. Murthy et al. (2006) used the magnetic data and concluded that the two significant E-W faults spanning from land to offshore north of Pondicherry and Vedaranyam control the Cauvery Basin. The coast near Baruva experienced lateral shifting along the E-W trending fault (Vaz et al., 1998). Neotectonic subsidence may explain the transgressed western shoreline of the Vasishta Godavari River mouth.

Some of the prominent faults are the Gundlamma Fault, Eocene Hinge Zone, Amaradakki Fault, Amirdi Fault, Attur Fault, Bhavani-Kanumudi Fault, Bhavanasi River Fault, Cauveri Fault, Javadi Hills Fault, Karkambadi-Swarnamukhi Fault, Kolleru Lake Fault, Pambar River Fault, Palar River Fault, Rajamatam-Point Calimere Fault, Tirukkavilur-Pondicherry Fault, Tirumala Fault, Vaigai River Fault and Vasishta—Godavari Fault. Although the frequency of earthquakes is low on the East Coast, their impact on society is high. The occurrence of moderate shallow-depth intraplate earthquakes has created concern in the scientific communities, leading to an understanding of the transformation of seismic activity along the East Coast (Rai et al., 2015).

## Data and methodology

### Data

We used open-source spatial and non-spatial data to assess the earthquake risk of the east coast region (Fig. 2). The earthquake inventory starting from the year 1900 to 2022 was accumulated from the National Centre of Seismology, Government of India (<https://seismo.gov.in/>). The geological features like faults and lithology were downloaded from the Bhukosh GSI (<https://bhukosh.gsi.gov.in/>) and the Universität Hamburg (Gleeson et al., 2011), respectively. The Peak Ground Acceleration (PGA) was calculated by applying the global relations developed by Caprio et al. (2015). The spatial sediment thickness dataset has been acquired from the Food and Agricultural Organization, United Nations (Fischer et al., 2008), whereas the time-averaged shear-wave velocity to 30 m depth ( $V_{s30}$ )

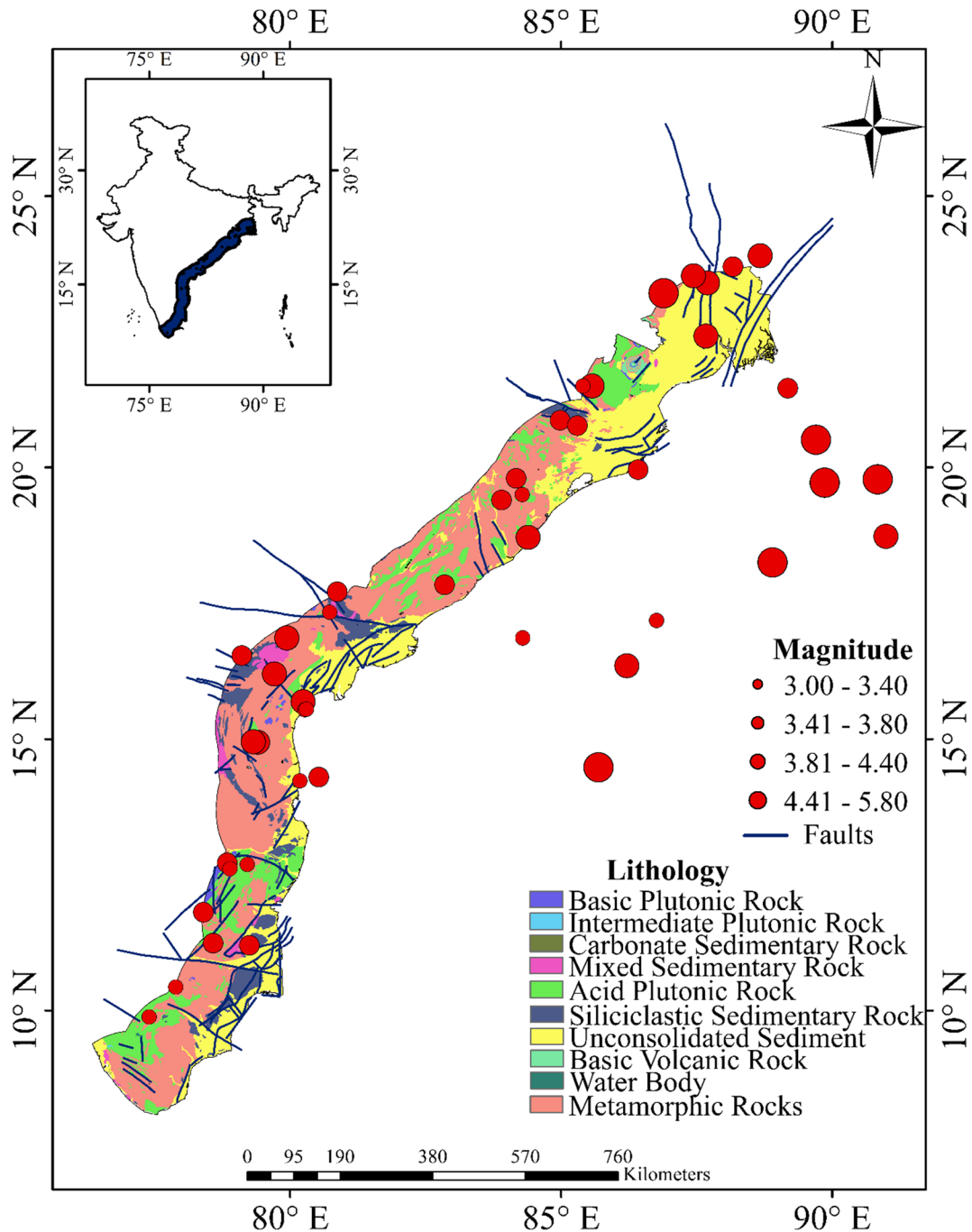


**Fig. 1** Location of the study area. Also, referenced are earthquakes, lithology, and significant faults

parameters were collected from the United States Geological Survey (Worden et al., 2015). The shuttle radar topography mission (NASA Shuttle Radar Topography Mission, SRTM, 2013) elevation data has been utilised to map the earthquake risk. The dataset of the different

infrastructures, administrative boundaries, land use and land cover was acquired from various open sources, including OpenStreetMap (<https://www.openstreetmap.org/>) and DIVA-GIS (<https://www.diva-gis.org/>). We have applied buffering of one degree of latitude

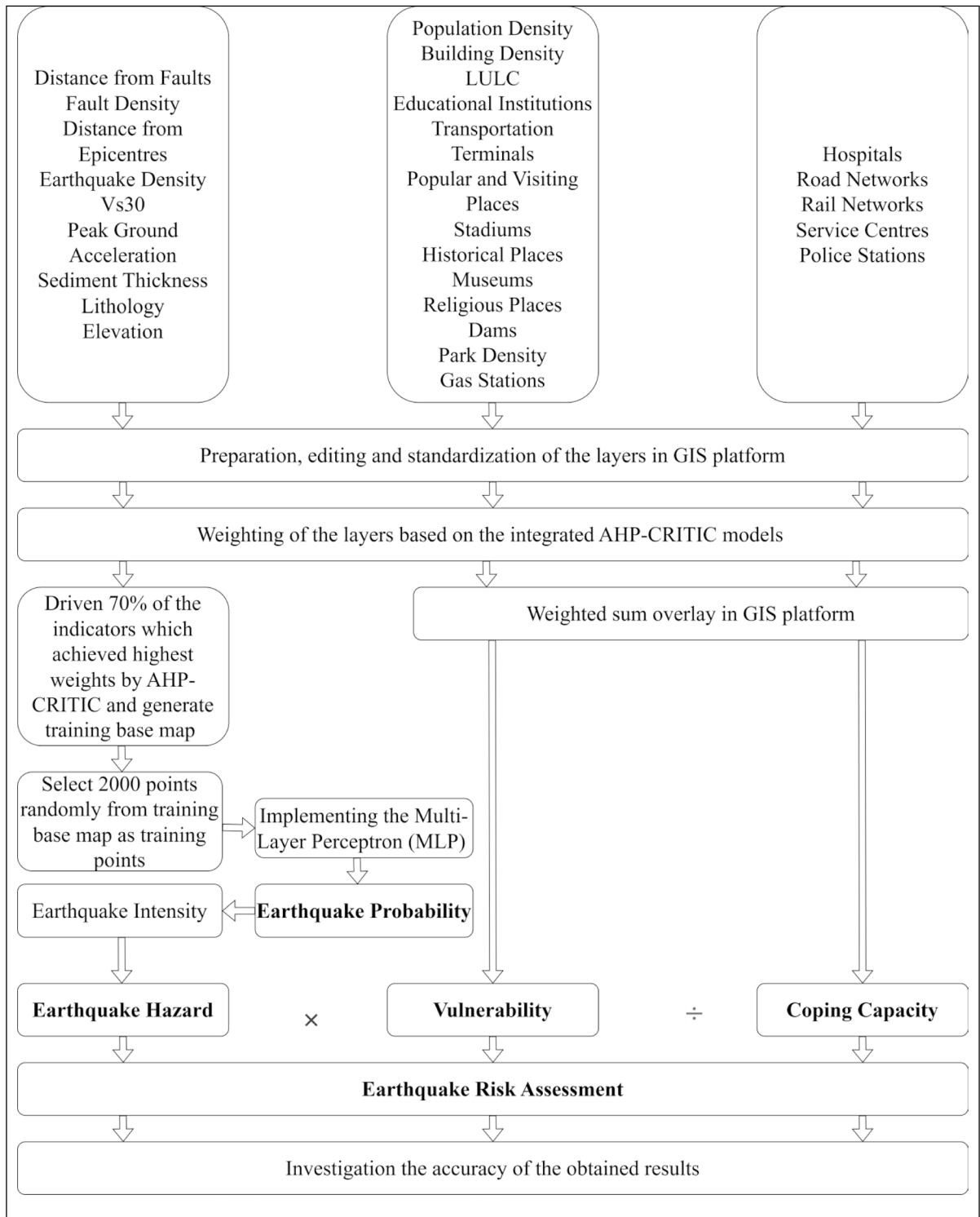


**Fig. 2** Flowchart illustrating the method adopted to compute risk for the study area

(nearly 110 km) to generate the western boundary. To convert non-spatial (or point data) datasets to spatial ones, we have applied inverse distance weighting to estimate spatial peak ground acceleration in the study region. Euclidian distance has been used to calculate the distance from faults, epicentres, transportation terminals, stadiums, historical places, museums, gas stations, hospitals, road and rail networks, service centres and police stations. Subsequently, Kernel density algorithms have been utilised to estimate the density of faults, population, buildings, educational institutions, popular and visiting places, religious places, dams and parks. The LULC and lithology have been directly converted into raster format using a data conversion tool. The impact of the chosen parameters on the earthquake risk assessment is explained in detail by Malakar et al. (2022). The resolution of the spatial layers is 30 m (rows, columns=56,239, 45,539), and the datasets were last accessed on January 25th 2023. In the next section, we have discussed the proposed methodology in detail.

#### Integration of AHP-CRITIC

In 1980, Saaty developed the subjective multi-criteria decision-making (MCDM) model and named it the Analytic Hierarchy Process (AHP). This technique can help handle complex problems by employing a series of pairwise comparison matrices and further evaluating the priority of the criteria by a hierarchical structure. The developed matrices incorporate the experts' opinions and the available literature. Constructing the pairwise comparison matrix with the scores given to the criterion is the first step in this method. Based on the opinion and published literature, the user can be assigned a criteria score from 1 to 9 (Saaty, 1980). Then the developed matrix is normalised, and the priority of the criteria is evaluated. The consistency of the generated result can be checked using the consistency index (CI) and consistency ratio (CR) and calculated using the following equation:

$$CI = \frac{\lambda_{\max} - n}{n - 1} \text{ and } CR = \frac{CI}{RI}$$

where  $\lambda_{\max}$  is the principal eigenvalue, and  $n$  represents the number of used criteria. Saaty (1980) estimated the randomness indicator (RI). In the case of the  $CR < 0.1$ , then an acceptable consistency level for evaluating the priority of the criteria ( $w_i$ ) is achieved.

Diakoulaki et al. (1995) developed the objective CRITERIA Importance Through Inter-criteria Correlation (CRITIC) method. CRITIC measures contrast and conflict as a decision-making problem (Diakoulaki et al., 1995). The steps followed in the CRITIC calculation are mentioned below (Madic & Radovanović, 2015).

Firstly, the developed matrix has been normalised using the following equation: -

$$x_{ij}^* = \frac{x_{ij} - \min(x_{ij})}{\max(x_{ij}) - \min(x_{ij})}$$

where  $x_{ij}^*$  represents the normalised value of  $i^{\text{th}}$  alternative on  $j^{\text{th}}$  criterion.

The criterion's standard deviation and its correlation with other criteria are required to estimate the criteria weights. The weight of the  $j^{\text{th}}$  criterion ( $w_j$ ) is evaluated as:

$$w_j = \frac{C_j}{\sum_{j=1}^n C_j}$$

where  $C_j$  indicates the quantity of information contained in the  $j^{\text{th}}$  criterion, and formulated as:

$$C_j = \sigma_j \sum_{j'=1}^n (1 - r_{jj'})$$

where  $\sigma_j$  represents the standard deviation of the  $j^{\text{th}}$  criterion and  $r_{jj'}$  indicates the correlation coefficient. Diakoulaki et al. (1995) concluded that the given criterion provides a more significant amount of information with a higher value of  $C_j$ .

The final weight of the criteria is obtained by integrating the weight obtained from the AHP and CRITIC. The AHP weights are derived from field experts' opinions and published literature (Saaty, 1980); in contrast, the CRITIC is entirely based on the relationships (Diakoulaki et al., 1995). It might happen that the experts, whilst calculating the AHP weight, usually ignore the data information, leading to uncertainty (Rodcha et al., 2019), whereas the weights estimated by the CRITIC are sometimes different from reality (Krishnan et al., 2021). To solve this discrepancy, Chuansheng et al. (2012) computed a formula to estimate the overall weight ( $w$ ) that considers the subjective and objective weights. In this study, the subjective weights are estimated using AHP, and the objective weights have been evaluated using CRITIC. The formula for the overall weight can be written as follows:

$$w = \alpha w_i + (1 - \alpha)w_j$$

where  $0 \leq \alpha \leq 1$ ; for the actual condition, the value  $\alpha$  set to 0.6 (Chuansheng et al., 2012). After the calculation of the final weights of each parameter, we applied the weighted sum tool in the GIS platform to develop the final output. This integrated method has been used to estimate earthquake vulnerability and coping capacity (Tables 1, 2). Furthermore, this methodology has been implemented to develop the training base map to evaluate the earthquake probability through an artificial neural network (ANN) discussed in the subsequent sections.

### Artificial neural network (ANN)

ANN is a computing model that can conclude linear or non-linear relations between variables in input and output datasets (Hagan et al., 1996). The ANN outcompetes the statistical methods in accuracy (Zhang et al., 1998). As a result, high accuracy can be obtained when using ANN for the earthquake probability assessment (Malakar et al., 2022; Yariyan et al., 2020). However, optimal training and network architecture are still unknown (Sözen, 2009). Trial and error are popular approaches researchers apply, outperforming other methods accuracy-wise (Lynch et al., 2001).

The most common ANN is the multilayer perceptron (MLP) network. MLP neural networks are simple, flexible and well-described by many researchers (Alizadeh et al., 2018; Yariyan et al., 2020). ANN neurons weighted to other layers process information independently (Ajith, 2005). In an MLP network, the backpropagation algorithm is applied to reduce the error (Salarian et al., 2014). Hence, we used the backpropagation algorithm to train the MLP. Training data is used by the learning algorithm to link input and output layers. The test dataset validates the trained network. So, we must select and prepare the training site parameter properly, influencing the result's accuracy (Malakar et al., 2022).

### Implementation of AHP-CRITIC with ANN

Nine spatial datasets mapped East Coast earthquake probability. To prepare a proper training database for the ANN model, we used the AHP-CRITIC integrated method. First, for the base map created in the GIS platform, seventy per

cent of the highest weighted parameters resulting from the AHP-CRITIC were utilised. Subsequently, 2000 points were selected, characterised as earthquake and non-earthquake points from the base map to the final training site map. We obtained and classified the entire earthquake catalogue from 1900 to 2022 as earthquake points from the National Institute for Seismology, Government of India. These points were utilised in feedforward MLP training to assess network accuracy. The final output is standardised and categorised into five classes. Backpropagation reduced error and assessed model root mean square error (RMSE). Subsequently, the resulting map was transferred to the GIS platform for earthquake hazard assessment. Tables 3, 4 and 5 show data, network structure, training parameters, the confusion matrix and the Kappa Index of Agreement between classified and predicted maps for each class for the ANN methodology. The details of the calculation of user and producer accuracy and the Kappa index of the agreement have been given by Ngoy et al. (2021).

### Hazard and risk

The hazard map for the east coast was created using earthquake probability and intensity variation spatial information (Jena et al., 2021b; Malakar et al., 2022). The intensity variation was estimated using the intensity value based on the magnitude of the events and then interpolating them. Following that, the intersection theory was applied, and the hazard zones were classified based on the quantile classification technique (Jena et al., 2021b). Finally, spatial information on the vulnerability, earthquake hazards and coping capacity is used to estimate the earthquake risk for the eastern coast of India. The mathematical formulation of the risk is the following:

$$\text{Risk} = \frac{\text{Vulnerability} \times \text{Hazard}}{\text{Coping capacity}}$$

## Results and discussions

### Vulnerability

The parameters used to estimate the vulnerability and the decision matrix with weights calculated using the AHP-CRITIC have been tabulated in Table 1. The population density achieved the higher weight,

**Table 1** Priority estimation of the parameters for vulnerability

	1	2	3	4	5	6	7	8	9	10	11	12	13
1	1	2	2	3	3	3	4	5	5	7	7	8	9
2	1/2	1	2	2	3	3	4	4	5	5	7	7	8
3	1/2	1/2	1	2	2	3	3	4	4	5	5	6	7
4	1/3	1/2	1/2	1	2	2	3	3	4	4	5	6	7
5	1/3	1/3	1/2	1/2	1	2	2	3	3	4	4	5	6
6	1/3	1/3	1/3	1/2	1/2	1	2	2	3	3	4	5	6
7	1/4	1/4	1/3	1/3	1/2	1/2	1	2	2	3	3	4	5
8	1/5	1/4	1/4	1/3	1/3	1/2	1/2	1	2	2	3	4	5
9	1/5	1/5	1/4	1/4	1/3	1/3	1/2	1/2	1	2	2	3	3
10	1/7	1/5	1/5	1/4	1/4	1/3	1/3	1/2	1/2	1	2	2	3
11	1/7	1/7	1/5	1/5	1/4	1/4	1/3	1/3	1/2	1/2	1	2	3
12	1/8	1/7	1/6	1/6	1/5	1/5	1/4	1/4	1/3	1/2	1/2	1	2
13	1/9	1/8	1/7	1/7	1/6	1/6	1/5	1/5	1/3	1/3	1/3	1/2	1

$$CR = 3.2\%$$

$$\lambda_{max} = 13.590$$

Sl. No.	Layers	AHP Weight	CRITIC Weight	Final Weight
1	Population Density (per km <sup>2</sup> )	20.90%	07.50%	15.54%
2	Building Density (per km <sup>2</sup> )	17.10%	11.10%	14.70%
3	LULC	13.60%	10.80%	12.54%
4	Education Institution (per degree <sup>2</sup> )	11.00%	07.80%	09.72%
5	Transportation Terminal (km)	08.70%	07.90%	08.38%
6	Visiting and Popular Places (per degree <sup>2</sup> )	07.20%	09.40%	08.08%
7	Stadium (km)	05.50%	06.80%	06.02%
8	Historical Places (km)	04.50%	05.90%	05.06%
9	Museum (km)	03.40%	07.40%	05.00%
10	Religious Places (per degree <sup>2</sup> )	02.70%	05.50%	03.82%
11	Dams (per degree <sup>2</sup> )	02.20%	06.20%	03.80%
12	Park Density (per degree <sup>2</sup> )	01.70%	06.80%	03.74%
13	Gas Station (km)	01.30%	07.10%	03.62%



**Table 2** Priority estimation of the parameters for coping capacity

	1	2	3	4	5
1	1	2	3	4	5
2	1/2	1	2	3	4
3	1/3	1/2	1	2	3
4	1/4	1/3	1/2	1	2
5	1/5	1/4	1/3	1/2	1

$$CR = 1.5\%$$

$$\lambda_{max} = 5.068$$

Sl. No.	Layers	AHP Weight	CRITIC Weight	Final Weight
1	Hospital (km)	41.90%	23.90%	34.70%
2	Road Network (km)	26.30%	20.10%	23.82%
3	Rail Network (km)	16.00%	12.60%	14.64%
4	Service Centre (km)	09.70%	18.00%	13.02%
5	Police Station (km)	06.20%	25.40%	13.88%

followed by the building density, whereas the gas station is the lowest priority, which is a secondary parameter. The major coastal cities were marked on the figure for reference (Fig. 3). Chennai, the capital city of Tamil Nadu, comes under the high vulnerable zone primarily due to high population counts. Haldia, Amravati and Kanyakumari fall under the moderately vulnerable area. Bhubaneswar and Puri, the major coastal cities of Odisha, Visakhapatnam of Andhra Pradesh and Pondicherry, come under the low vulnerable zone. Balasore and Thoothukudi reside under a very low vulnerability region.

The high population density in metropolitan cities, high building density, unmanaged land usage,

shortage of resources and non-homogeneous dispersion of transportation terminals and educational institutions could all contribute to high vulnerability (Malakar et al., 2022). For instance, Chennai comes under the high vulnerable zone primarily due to high population counts. From 2001 to 2011, the population of Chennai had decadal growth of 6.8%, with a population density of 26,553 (Census, 2011) and is considered the fourth-most densely populated Indian city. This city converted most agricultural lands into industrial and residential infrastructures due to rapid urbanisation. It is also estimated that India has the highest total coastal population exposure in the baseline year, which is expected to remain largely

**Table 3** Parameters and stopping criteria for implementing the MLP model

Group	Parameter	Value
Input specifications	Training points	2000
	Hidden layers	1
Network architecture	Nodes	7
	Input layers node	9
	Output layers node	5
	Activation function	Sigmoid
Training parameters	Automatic training	Yes
	Shuffle	Yes
	Learning rate initialisation	0.001
	Momentum factor	0.5
	Early stopping	Yes
Stopping criteria	RMSE	0.2617
	Iterations	10,000

unchanged, making the region more vulnerable. Compared to rural areas, metropolitan cities are more densely populated. Rural people usually migrate to these cities for better livelihood or due to harsh climatic conditions in higher elevations. They typically construct traditional non-engineered shelters due to a lack of resources, making this region more vulnerable (Asadi et al., 2019). Low-to-very vulnerability zones have good socioeconomic conditions and are usually not close to high-magnitude earthquake locations (Jena et al., 2021b).

About 25.30% of the east coast region area has been considered very low vulnerable, 43.86% has a low vulnerability, 21.74% has a moderate vulnerability, and 7.13% has a high vulnerability, with the remainder having a very high vulnerability.

**Table 4** Confusion matrix of the MLP model

Predicted		Very Low	Low	Moderate	High	Very High	Total	User Accuracy
Classified	Very low	109,723,464	2,432,678	0	0	0	112,156,142	97.83%
	Low	3,053,317	752,288,523	181,589,102	252,168	0	937,183,110	80.27%
	Moderate	0	122,994,887	291,844,842	293,961	9703	415,143,393	70.30%
	High	0	278,663	360,745	75,308,914	11,175,110	87,123,432	86.44%
	Very high	0	0	12,836	17,713,160	991,735,748	1,009,461,744	98.24%
	Total	112,776,781	877,994,751	473,807,525	93,568,203	1,002,920,561	2,561,067,821	
<b>Producer accuracy</b>		97.29%	85.68%	61.60%	80.49%	98.88%		<b>Overall accuracy = 86.72%</b>

In comparison, approximately 12.29% population resides in a very low earthquake-vulnerable zone, 32.81% is low, 25.72% is moderate and 29.18% is in high to very high earthquake vulnerability (Table 6). Thus, a significant part of the East Coast population are vulnerable to hazards. Therefore, the hazard mitigation organisations should prioritise the highly vulnerable regions.

**Earthquake hazard and risk**

By integrating AHP-CRITIC and ANN, the earthquake probability is estimated (Fig. 4), and this information with intensity variation has been used to assess the earthquake hazard. The parameters included in calculating the earthquake probability map were historical seismicity, geological features,  $V_{s30}$ , PGA and elevation. The hazard map indicates that Haldia falls under high hazardous regions. Bhubaneswar and Amravati lie under the moderate hazardous zone, whereas Pondicherry, Visakhapatnam

**Table 5** Kappa Index of Agreement between classified and predicted map for each class

	Classified	Predicted
Classes	Kappa Index of Agreement (%)	Kappa Index of Agreement (%)
Very	96.84	96.06
Low	71.28	79.16
Low	56.77	44.10
Moderate	80.26	71.60
High	97.44	98.38
Overall Kappa Index of Agreement = 80.67%		

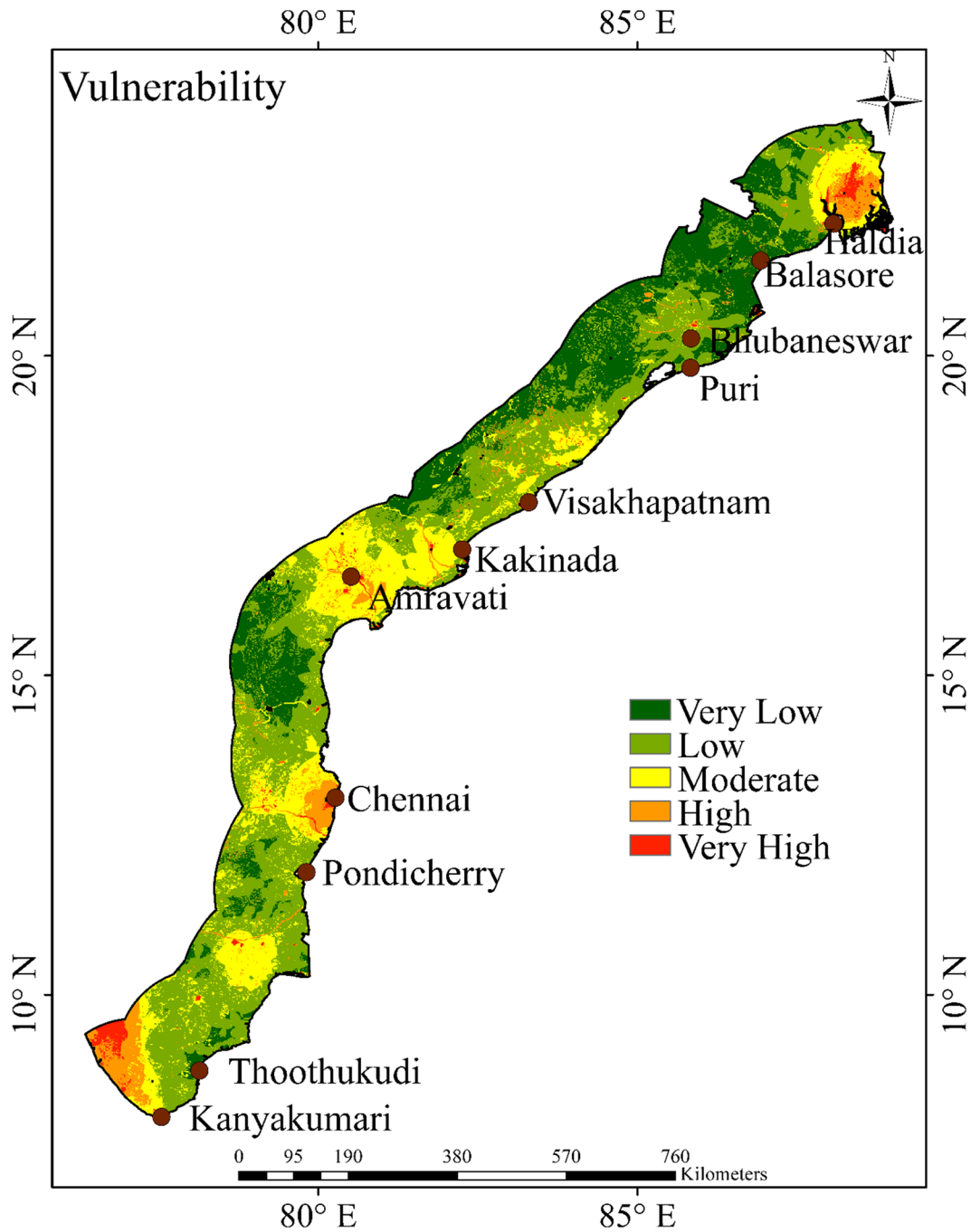


**Fig. 3** Vulnerability map for the eastern coastal plain of India. Red zones are highly vulnerable, while green zones are relatively low vulnerable

and Puri were included in the low hazard region (Fig. 5). Balasore, Kakinada and the southernmost point of India, Kanyakumari, fall in the very low earthquake zone.

The active faults, folds, dynamic lithology and geological features and several moderate earthquake events contribute to the probability of the east coast region. Haldia region is surrounded by the Eocene

**Table 6** Vulnerability, hazard and risk to earthquake based on population and areas

	Classes	Area %	Population %
Vulnerability	Very low	25.30	12.29
	Low	43.86	32.81
	Moderate	21.74	25.72
	High	07.13	12.06
	Very high	01.98	17.12
Earthquake hazard	Very low	28.54	27.58
	Low	14.97	12.67
	Moderate	23.65	19.60
	High	27.38	33.59
	Very high	05.46	06.57
Earthquake risk	Very low	29.89	27.48
	Low	36.25	32.09
	Moderate	29.40	29.19
	High	04.21	11.23
	Very high	00.25	00.01

Hinge Zone, the Pingla Fault and the Garhmoyna-Khandaghosh Fault. The Eocene Hinge Zone is a prominent NE-SW trending tectonic feature in the Bengal basin. In the last 350 years, near and far source earthquakes have caused damage in Haldia, with thirty strong earthquakes reported in the Bengal basin. The majority of earthquakes that surround Haldia are from distant locations, whilst two notable near-source earthquakes greatly impacted Haldia on September 29th 1906 and April 15th 1964 (Mohanty & Wallings, 2008). The 1964 earthquake occurred south of Haldia and is located over the Eocene Hinge Zone (GSI, 2000), which induced more damage to this region. Bhubaneswar and Amravati lie under the moderate hazardous zone. Bhubaneswar was located in seismic zone III, with an MSK intensity of VII and an expected maximum PGA of 0.16 g (IS 1893, 2002). Dhar et al. (2017) concluded that in the Bhubaneswar region, there are fewer earthquakes, and only neo-tectonic faults have lower influences on seismic hazards. Similarly, Amravati lies in seismic zone III and is categorised into low to moderate-risk zones due to earthquakes (IS 1893, 2002). Satyanarayana and Rajesh (2021) estimated that the maximum potential earthquake within Amaravati is about 6.7-moment magnitude. Pondicherry and Visakhapatnam have been recognised as zones of weakness with established neotectonic activity (Murthy et al., 2010).

We also find that 28.54% area is classified as very low hazard, 14.97% as low, 23.64% as moderate, 27.38% as high and 5.46% as very high. 27.58% of the population resides in a very low hazard zone, 12.67% in a low hazard zone, 19.60% in a moderate zone, 33.59% in a high zone, and the remaining resides in a very high hazardous zone (Table 6).

The earthquake risk map uses spatial hazard information, vulnerability and coping capacity. The analysis shows that significant metropolitan cities such as Puri, Kakinada, Chennai and Kanyakumari lie in the very low-risk zone (Fig. 6). Bhubaneswar, Visakhapatnam and Pondicherry fall under the low earthquake-risk zone, and Haldia and Amravati are included under the moderate risk area.

The numerical figures reveal that 29.89% of the east coast region has a very low earthquake risk, 36.25% has a low earthquake risk, 29.40% has a moderate earthquake risk, 4.21% has a high earthquake risk, and 0.25% has a very high earthquake risk. The population follows a similar pattern, with 27.48% of the population in the eastern coastal plain being under very low earthquake risk, 32.09% being low, 29.19% being moderate, 11.23% being high and a negligible percentage living in very high earthquake risk regions.

### Coping capacity

During earthquake events, coping capacity is a game-changer (Jena et al., 2021b). Coping capacity necessitates proper training, awareness and resource management. The coping capacity of the east coast has been determined using information regarding communication networks, hospitals, service centres and police stations. The AHP-CRITIC approach is applied to compute the weights of the factors (Table 2). The result indicates that most significant metropolitan cities fall under very high coping capacity except Balasore, which falls under moderate coping capacity (Fig. 7).

The result indicates that most significant metropolitan cities fall under very high coping capacity because of the development of several multispeciality governments, private hospitals, communication networks and disaster management centres (Fig. 7). These cities are relatively developed and pose a high coping capacity. However, the agencies should focus on areas with low coping capacity against the hazard.

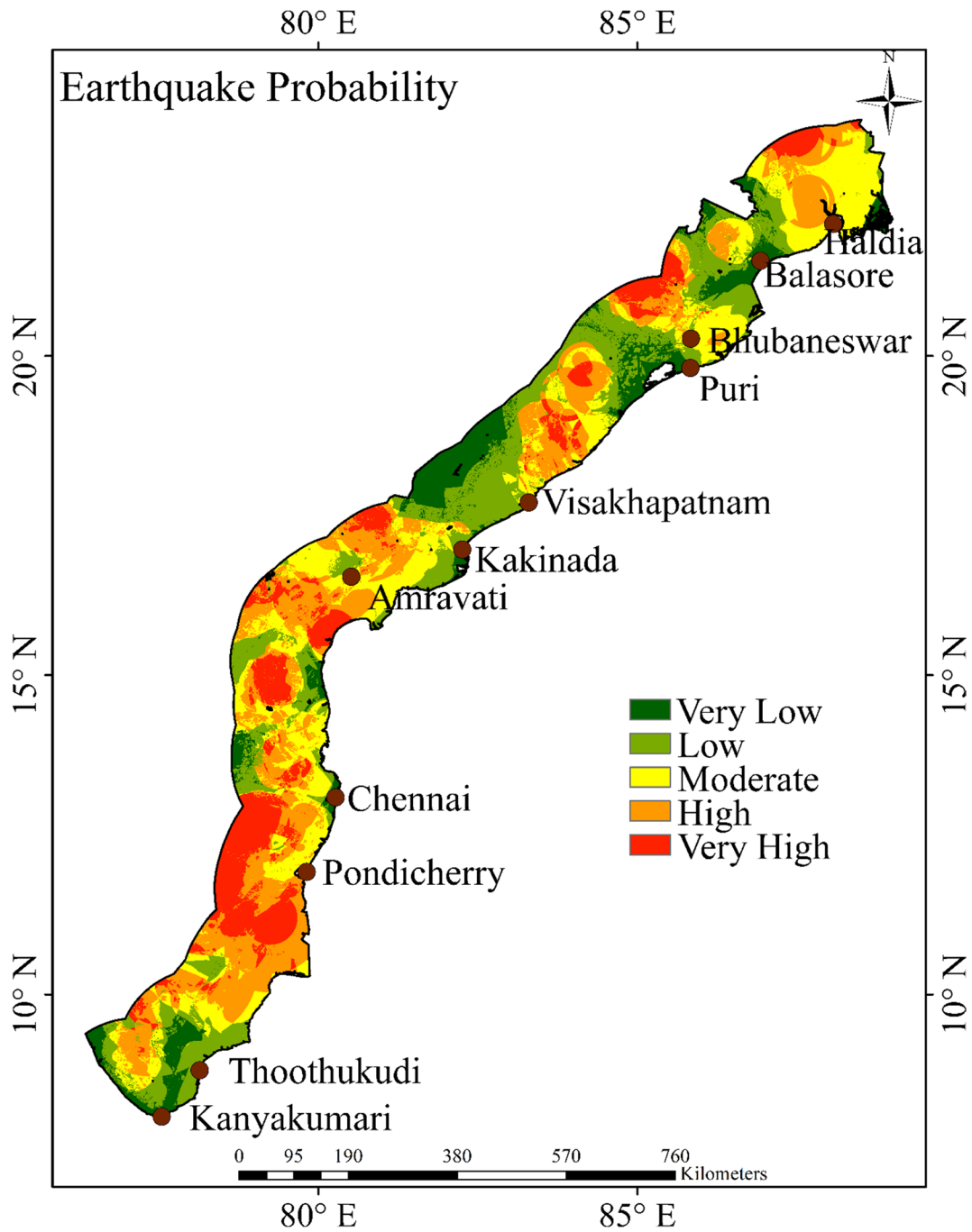


**Fig. 4** Earthquake probability map for the eastern coastal region of India

Interestingly, in the study area, less than 0.3% of the population has a very low coping capacity, 3.08% has a low, 9.30% has a moderate, 22.63% has a high and 64.73% has a very high coping capacity against the earthquake hazard. Nonetheless, approximately

12% population in the study area is at high seismic risk. However, these areas could be transformed into low-risk zones with appropriate planning and mitigation strategies.

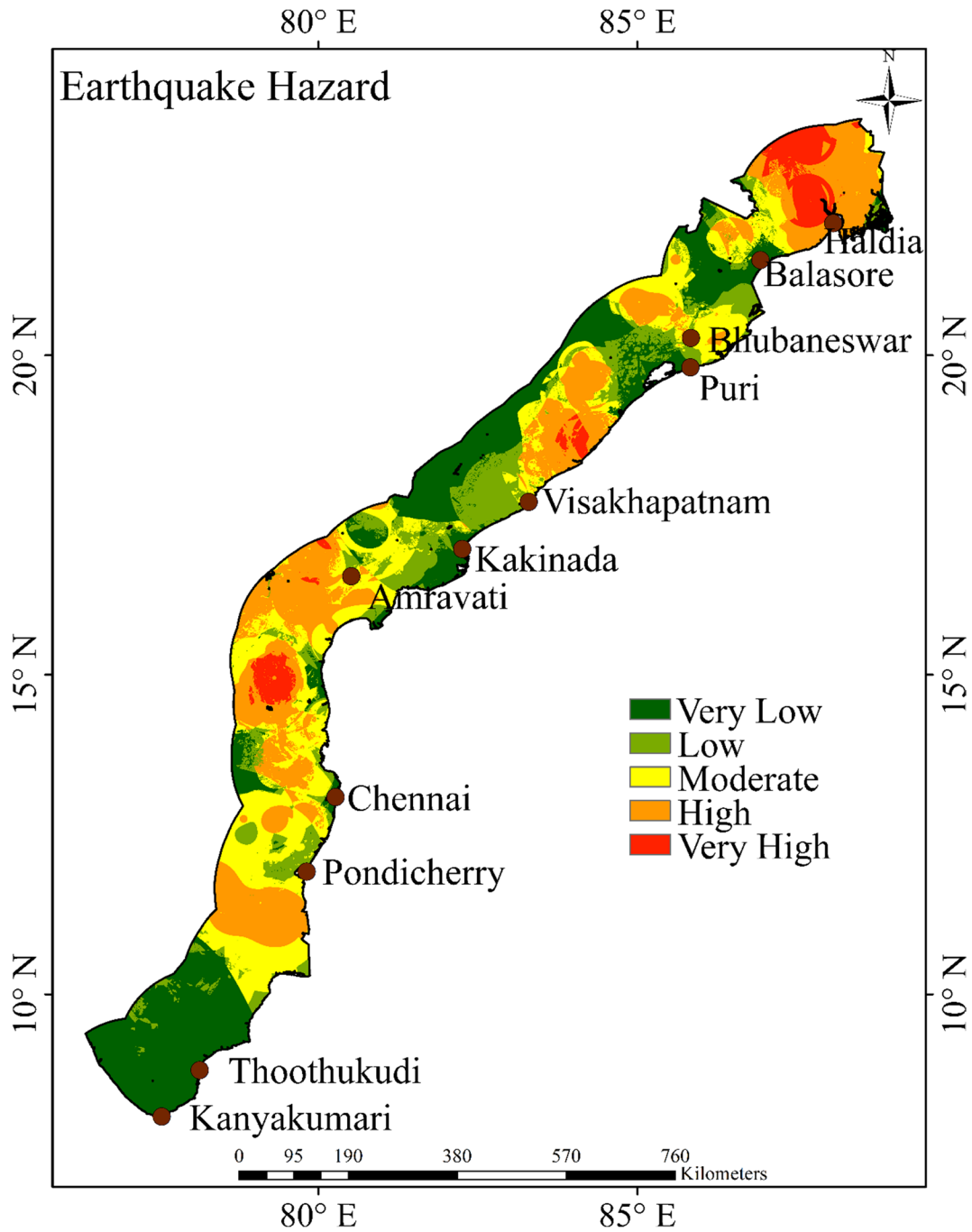


**Fig. 5** Earthquake hazard map for the eastern coastal region of India

Validation and sensitivity analysis of the model

We aim to develop a novel methodology that will improve estimations of the earthquake risk in the eastern coastal plain of India. We analysed vulnerability and

coping capacity sensitivity to comprehend the impact of parameters (Table 7). For this purpose, we determine the priority of the parameters by changing the alpha ( $\alpha$ ) value. The parameter used for the vulnerability has a consistent ranking for  $\alpha \geq 0.6$ , satisfying the results of

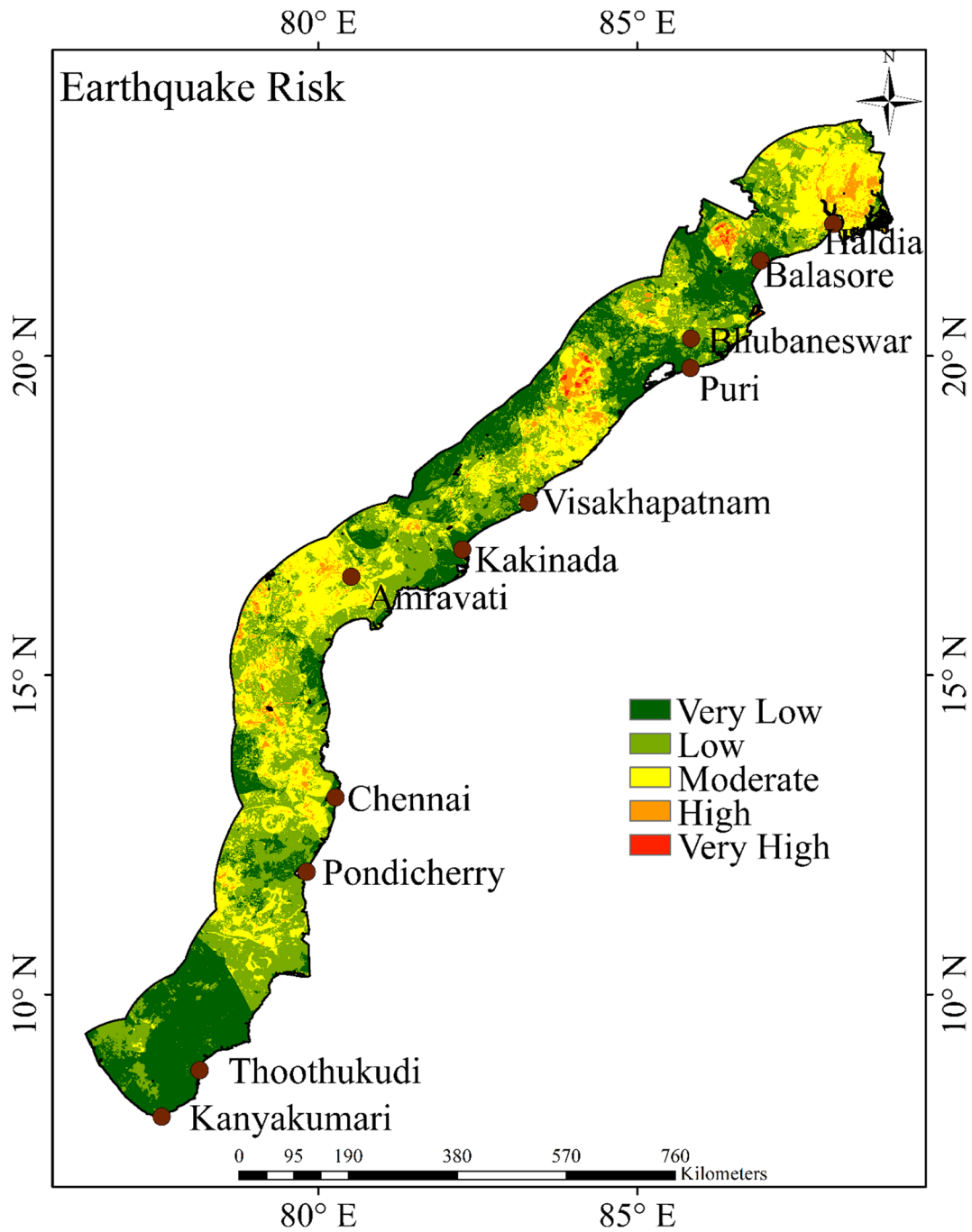


**Fig. 6** Earthquake risk map for the eastern coastal region of India. Red zones are very high risk, while green zones are relatively low risk zones

Chuansheng et al. (2012) that the value should be set as 0.6 for the actual situation of parameters. For the coping capacity, the sensitivity analysis indicates that when  $\alpha$  is 0.2, the hospital is at a higher priority and remains

throughout the analysis without the influence of  $\alpha$ . For  $\alpha=0.6$ , the ranking pattern becomes almost consistent except for service centres and police stations. For values of  $\alpha$  as 0.8 and 1, the ranking pattern remains consistent.

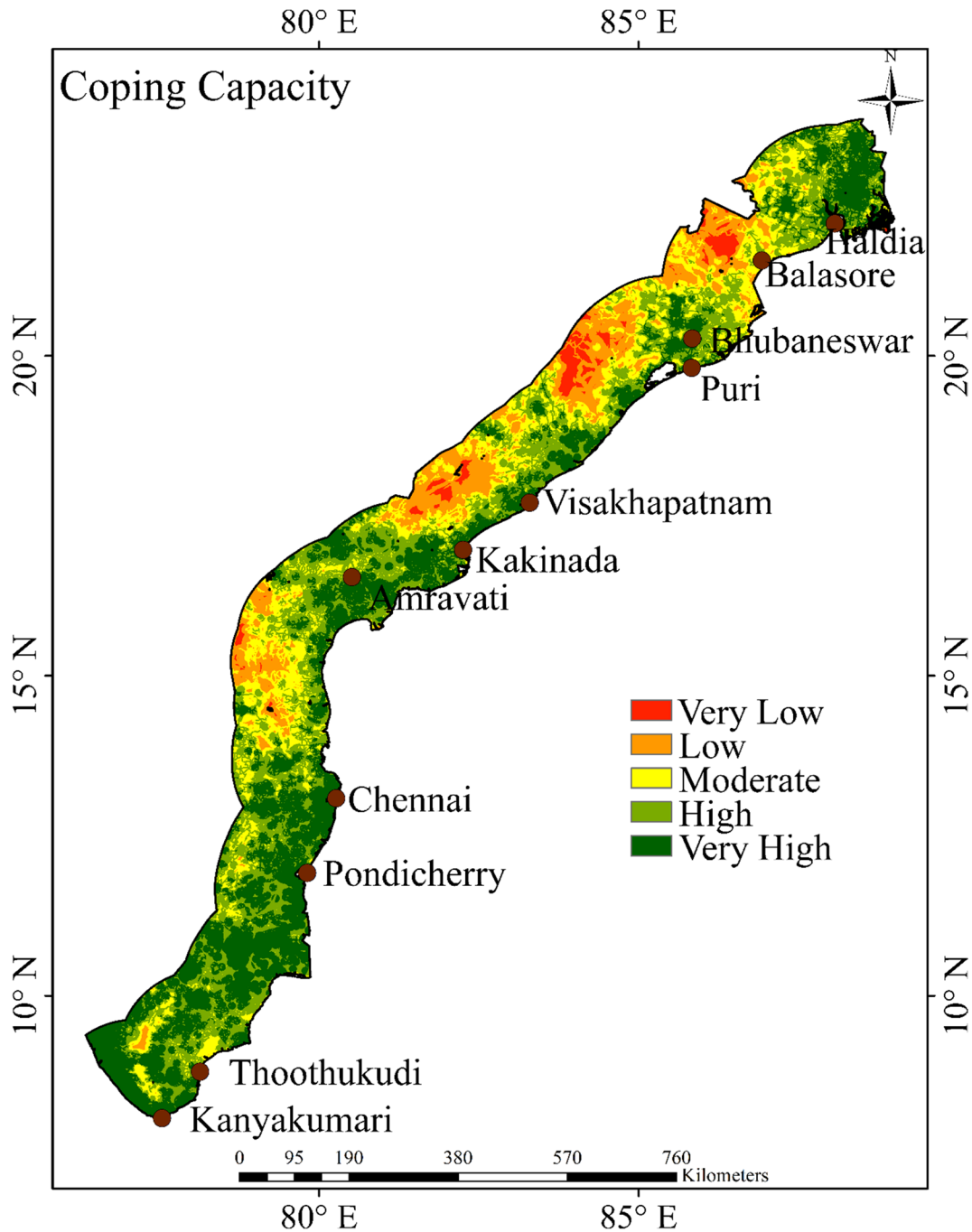


**Fig. 7** Coping capacity map for the eastern coastal region of India. Red zones have a very low coping capacity, while green zones have a relatively high coping capacity

Therefore, the sensitivity analysis validates our weight assigning and ranking procedure.

The confusion matrix yielded an overall accuracy of 86.72% (Table 4). The producer accuracy was high for all

the classes; however, the moderate class showed relatively lower accuracy. The user accuracy also exhibited the same pattern. The Kappa index of agreement exhibited a high value, reaching an overall index value of 80.67% (Table 5).



**Table 7** Sensitivity analysis of the applied MCDM model for vulnerability and coping capacity

Layers	$\alpha=0.2$	$\alpha=0.4$	$\alpha=0.6$	$\alpha=0.8$	$\alpha=1$
Population density	0.1018 (3)	0.1286 (2)	0.1554 (1)	0.1822 (1)	0.2090 (1)
Building density	0.1230 (1)	0.1350 (1)	0.1470 (2)	0.1590 (2)	0.1710 (2)
LULC	0.1138 (2)	0.1196 (3)	0.1254 (3)	0.1312 (3)	0.1370 (3)
Education institution	0.0844 (5)	0.0908 (4)	0.0972 (4)	0.1036 (4)	0.1100 (4)
Transportation terminal	0.0806 (6)	0.0822 (6)	0.0838 (5)	0.0854 (5)	0.0870 (5)
Visiting and Popular Places	0.0896 (4)	0.0852 (5)	0.0808 (6)	0.0764 (6)	0.0720 (6)
Stadium	0.0654 (8)	0.0628 (7)	0.0602 (7)	0.0576 (7)	0.0550 (7)
Historical places	0.0562 (9)	0.0534 (9)	0.0506 (8)	0.0478 (8)	0.0450 (8)
Museum	0.0660 (7)	0.0580 (8)	0.0500 (9)	0.0420 (9)	0.0340 (9)
Religious places	0.0494 (13)	0.0438 (13)	0.0382 (10)	0.0326 (10)	0.0270 (10)
Dams	0.0540 (12)	0.0460 (12)	0.0380 (11)	0.0300 (11)	0.0220 (11)
Park density	0.0578 (11)	0.0476 (11)	0.0374 (12)	0.0272 (12)	0.0170 (12)
Gas station	0.0594 (10)	0.0478 (10)	0.0362 (13)	0.0246 (13)	0.0130 (13)
Layers	$\alpha=0.2$	$\alpha=0.4$	$\alpha=0.6$	$\alpha=0.8$	$\alpha=1$
Hospital	0.2750 (1)	0.3110 (1)	0.3470 (1)	0.3830 (1)	0.4190 (1)
Road network	0.2134 (3)	0.2258 (2)	0.2382 (2)	0.2506 (2)	0.2630 (2)
Rail network	0.1328 (5)	0.1396 (5)	0.1464 (3)	0.1532 (3)	0.1600 (3)
Service centre	0.1634 (4)	0.1468 (4)	0.1302 (5)	0.1136 (4)	0.0970 (4)
Police station	0.2156 (2)	0.1772 (3)	0.1388 (4)	0.1004 (5)	0.0620 (5)

In general, the model demonstrated a significantly high level of accuracy. Comparing our result with previous literature, Jena et al. (2020) found that the coastal areas of Odisha fall under a moderate to very low earthquake probability zone, indicating that these areas are not highly probable for future events, and our result is almost aligned with their outcome (Fig. 4). However, their methodology was different from our proposed model. The other validation method is to develop the receiver operating characteristic (ROC) curve and evaluate the model’s sensitivity to earthquake probability. The area under the curve (AUC) is a metric used to assess the accuracy of an earthquake probability assessment. Generally, the AUC has been categorised as no discrimination, acceptable, excellent and outstanding for values equal to 0.5, 0.7–0.8, 0.8–0.9 and greater than 0.9, respectively (Malakar et al., 2022). Our result shows an AUC value of 0.85, which is considered relatively good for validating the accuracy of our model. (Fig. 8) and makes our approach better for mapping the earthquake risk for the study area.

**Model limitations and future prospects**

The model’s strengths, challenges and weaknesses are based on the model data, thematic parameters and model implementation. This study aims to predict an earthquake risk on the east coast of India by using the

integrated combined MCDM methods (subjective and objective), along with the ANN and GIS techniques. This study show cases a thorough evaluation of risks and can be implemented on a large scale to obtain precise risk information.

The constraints and challenges of this study are mostly related to collecting large datasets and their processing using machine-learning algorithms. Proper datasets of some parameters may not be available, besides obtaining datasets for larger study regions. As a result, data from other (secondary) sources are used, which may contain inaccuracies. Similarly, absence of parameters such as liquefaction factors, soil characteristics, fault characteristics, earthquake precursors, seismic structure and building types has an impact on the study. Subjectivity makes it difficult to obtain high-quality data and estimate priorities. Furthermore, limitations also arise from failing to account for diurnal or day and night fluctuations in many characteristics when evaluating vulnerability. Also, the ANN technique is data-dependent. Hence, an earthquake probability distribution study requires lots of training data; selecting appropriate parameters is crucial to avoid bias in results. Designing and implementing the ANN model require a significant amount of work. Despite all these limits and obstacles, the models used in this study are effective for assessing

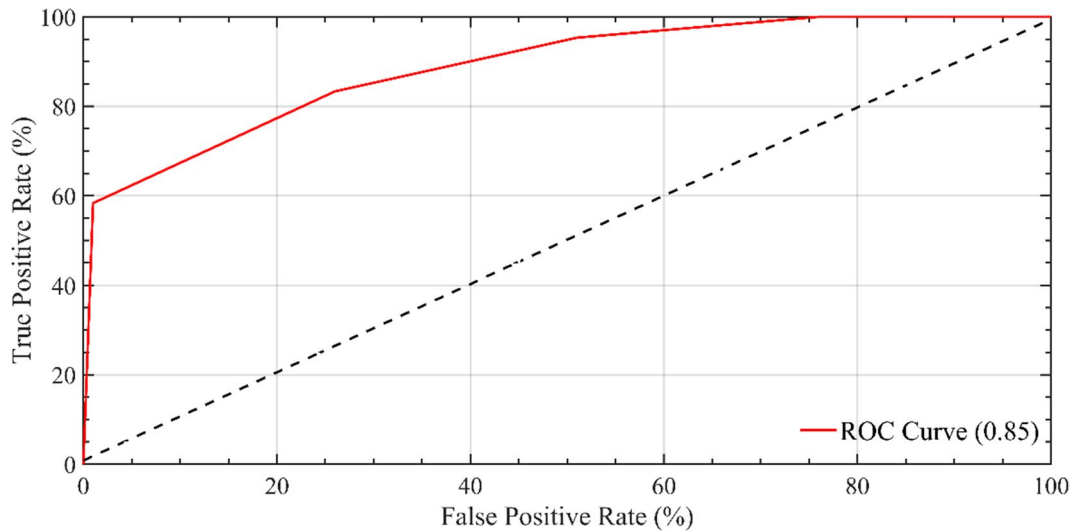


**Fig. 8** Receiver operating characteristic curve (ROC) for the earthquake probability map

earthquakes and mitigating and minimising disaster risk. This approach can be used in other areas with few modifications, and several government agencies can utilise the results.

However, high-resolution LiDAR-created Digital Elevation Models (DEMs) and a three-dimensional city model may improve results in the future. Additionally, future research should explore the impact of biodiversity on earthquake risk assessment in specific regions in conjunction with other machine-learning methods. Ultimately, the integration of the AHP, CRITIC and ANN with Geographic Information System (GIS) provides a promising framework for investigating the effects of various disasters on both society and infrastructure.

## Conclusions

Identifying hazardous and risk zones is a crucial aspect of mitigating seismic hazards. In this study, we have estimated the earthquake risk for the east coast of India by integrating MCDM models, namely the subjective AHP and the objective CRITIC, with ANN. Twenty-seven non-spatial and spatial data sets were used to evaluate earthquake risk in the study area.

This study indicates that approximately 4.46% of the area of the East Coast region is prone to high earthquake risk, 29.40% moderate, 36.25%

low risk, and the remaining area is under very low earthquake risk. About 11.24% of the total residing population is at high risk, 29.19% at moderate, 32.09% at low and 27.48% live under very low risk. The sensitivity analysis has been performed to comprehend the impact of various parameters used to develop the coping capacity and vulnerability for the east coast. We have also used the ROC curve to validate the AHP-CRITIC-ANN integrated model, which indicated relatively good results with an AUC of 0.85. The results may be helpful to mitigation and planning authorities in identifying risk prone areas in the East Coast region and plan for any potential earthquake induced disaster well in advance.

**Acknowledgements** The authors thank the Indian Institute of Technology Kharagpur, and the Ministry of Education, Government of India for supporting this work. We also thank various Institutes and organisations for providing the data used in this study available in the public domain.

**Author contribution** Abhishek K. Rai: methodology, investigation, resources, visualisation, writing—original draft, review and editing. Sukanta Malakar: investigation, data acquisition, writing—original draft. Susmita Goswami: investigation, writing—review and editing.

**Data availability** The data used in this study are freely available.

**Declarations**

**Ethics approval** All authors have read, understood and have complied as applicable with the statement on ‘Ethical responsibilities of Authors’ as found in the Instructions for Authors.

**Consent to participate** Not applicable.

**Consent for publication** All the authors are willing and have no conflict in publishing the article in this journal.

**Competing interests** The authors declare no competing interests.

## References

- Ajith, A. (2005). *Artificial neural networks*. Handbook of measuring system design. New York, John Wiley & sons.
- Alexander, D. (2018). Civil protection in Italy-coping with multiple disasters. *Contemporary Italian Politics*, 10, 393–406. <https://doi.org/10.1080/23248823.2018.1544354>
- Alizadeh, M., Ngah, I., Hashim, M., Pradhan, B., & Beiranvand, A. P. (2018). A hybrid analytical network process and artificial neural network (ANP-ANN) model for urban earthquake vulnerability assessment. *Remote Sensing*, 10(6), 975. <https://doi.org/10.3390/rs10060975>
- Asadi, Y., Samany, N. N., & Ezimand, K. (2019). Seismic vulnerability assessment of urban buildings and traffic networks using fuzzy ordered weighted average. *Journal of Mountain Science*, 16, 677–688. <https://doi.org/10.1007/s11629-017-4802-4>
- Banerjee, P. K., Vaz, G. G., Sengupta, B. J., & Bagchi, A. (2001). A qualitative assessment of seismic risk along peninsular coast of India, south of 19° N. *Journal of Geodynamics*, 31, 481–498. [https://doi.org/10.1016/S0264-3707\(01\)00030-8](https://doi.org/10.1016/S0264-3707(01)00030-8)
- Bhattacharya, A., Geraghty, J., & Young, P. (2010). Supplier selection paradigm: An integrated hierarchical QFD methodology under multiple-criteria environment. *Applied Soft Computing*, 10, 1013–1027. <https://doi.org/10.1016/j.asoc.2010.05.025>
- Caprio, M., Tarigan, B., Worden, B. C., Wiemer, S., & Wald, D. J. (2015). Ground motion to intensity conversion equations (GMICES): A global relationship and evaluation of regional dependency. *Bulletin of the Seismological Society of America*, 105, 1476–1490. <https://doi.org/10.1785/0120140286>
- Census. (2011). *Primary census abstract 2011 - India and states*. Registrar general and census commissioner, department of home, ministry of home affairs, government of India.
- Chuansheng, X., Dapeng, D., Shengping, H., Xin, X., & Yingjie, C. (2012). Safety evaluation of smart grid based on AHP-entropy method. *Systems Engineering Procedia*, 4, 203–209. <https://doi.org/10.1016/j.sepro.2011.11.067>
- CRED. (2015). *The human cost of natural disasters: A global perspective, centre for research on the epidemiology of disaster(CRED)*.
- Dhar, S., Rai, A. K., & Nayak, P. (2017). Estimation of seismic hazard in Odisha by remote sensing and GIS techniques. *Natural Hazards*, 86, 695–709. <https://doi.org/10.1007/s11069-016-2712-3>
- Diakoulaki, D., Mavrotas, G., & Papayannakis, L. (1995). Determining objective weights in multiple criteria problems: The critic method. *Computers & Operations Research*, 22(7), 763–770. [https://doi.org/10.1016/0305-0548\(94\)00059-H](https://doi.org/10.1016/0305-0548(94)00059-H)
- Fischer, G., Nachtergaele, F., Prieler, S., Van Velthuizen, H. T., Verelst, L., & Wiberg, D. (2008). Global agro-ecological zones assessment for agriculture (GAEZ 2008). IIASA, Laxenburg, Austria and FAO, Rome, Italy, 10.
- Gleeson, T., Smith, L., Moosdorf, N., Hartmann, J., Dürr, H. H., Manning, A. H., van Beek, L. P. H., Jellinek, A. M. (2011). Mapping permeability over the surface of the Earth. *Geophysical Research Letters*, 38. <https://doi.org/10.1029/2010GL045565>
- GSI. (2000). *Seismotectonic Atlas of India and its environments, geological survey of india*.
- GSI. (2002). *Surface sea bed map off Chilka-I, Bay of Bengal, geological survey of india*.
- GSI. (2005). *Surface seabed map off Paradip, Bay of Bengal, geological survey of india*.
- Hagan, M. T., Demuth, H. B., & Beale, M. (1996). *Neural Network Design*. PWS Publishing.
- IS 1893. (2002). *Indian standard criteria for earthquake resistant design of structures, Part 1-General provisions and buildings*. Bureau of Indian Standards, New Delhi.
- Jena, R., Pradhan, B., Beydoun, G., Nizamuddin, A., Sofyan, H., & Afan, M. (2019). Integrated model for earthquake risk assessment using neural network and analytic hierarchy process: Aceh Province, Indonesia. *Geoscience Frontiers*, 11, 613–634. <https://doi.org/10.1016/j.gsf.2019.07.006>
- Jena, R., Pradhan, B., & Alamri, A. M. (2020). Susceptibility to seismic amplification and earthquake probability estimation using recurrent neural network (RNN) model in Odisha. *India. Applied Sciences*, 10, 15. <https://doi.org/10.3390/app10155355>
- Jena, R., & Pradhan, B. (2020). Integrated ANN-cross-validation and AHP-TOPSIS model to improve earthquake risk assessment. *International Journal of Disaster Risk Reduction*, 50. <https://doi.org/10.1016/j.ijdr.2020.101723>
- Jena, R., Pradhan, B., Beydoun, G., Alamri, A., & Shanableh, A. (2021a). *Spatial earthquake vulnerability assessment by using multi-criteria decision making and probabilistic neural network techniques in Odisha*. Geocarto International. <https://doi.org/10.1080/10106049.2021.1992023>
- Jena, R., Pradhan, B., Naik, S. P., & Alamri, A. M. (2021). Earthquake risk assessment in NE India using deep learning and geospatial analysis. *Geoscience Frontiers*, 12, 3. <https://doi.org/10.1016/j.gsf.2020.11.007>
- Karuppusamy, B., George, S. L., Anusuya, K., Venkatesh, R., Thilagaraj, P., Gnanappazham, L., Kumaraswamy, K., Balasundareswaran, A. H., & Nina, P. B. (2021). Revealing the socio-economic vulnerability and multi-hazard risks at micro-administrative units in the coastal plains of Tamil Nadu, India. *Geomatics, Natural Hazards and Risk*, 12, 605–630. <https://doi.org/10.1080/19475705.2021.1886183>

- Krishnan, A. R., Kasim, M. M., Hamid, R., & Ghazali, M. F. (2021). A modified CRITIC method to estimate the objective weights of decision criteria. *Symmetry*, *13*(6). <https://doi.org/10.3390/sym13060973>
- Lynch, M., Patel, H., Abrahamse, A., Rajendran, A. R., & Medsker, L. (2001). Neural network applications in physics. *International Joint Conference on Neural Networks*, *3*, 2054–2058. <https://doi.org/10.1109/IJCNN.2001.938482>
- Madic, M., & Radovanović, M. (2015). Ranking of some most commonly used nontraditional machining processes using ROV and CRITIC methods. *Scientific Bulletin-University Politehnica of Bucharest Series D*, *77*(2), 193–204.
- Malakar, S., & Rai, A. K. (2022a). Earthquake vulnerability in the Himalaya by integrated multi-criteria decision models. *Natural Hazards*, *111*, 213–237. <https://doi.org/10.1007/s11069-021-05050-8>
- Malakar, S., & Rai, A. K. (2022b). Seismicity clusters and vulnerability in the Himalayas by machine learning and integrated MCDM models. *Arabian Journal of Geosciences*, *15*, 1674. <https://doi.org/10.1007/s12517-022-10946-1>
- Malakar, S., & Rai, A. K. (2023). Estimating seismic vulnerability in West Bengal by AHP-WSM and AHP-VIKOR. *Natural Hazards Research*, *3*(3), 464–473. <https://doi.org/10.1016/j.nhres.2023.06.001>
- Malakar, S., Rai, A. K., & Gupta, A. K. (2022). Earthquake risk mapping in the Himalayas by integrated analytical hierarchy process, entropy with neural network. *Natural Hazards*, *116*, 951–975. <https://doi.org/10.1007/s11069-022-05706-z>
- Malakar, S., Rai, A. K., Kannaujia, V. K., & Gupta, A. K. (2023). Revised empirical relations between earthquake source and rupture parameters by regression and machine learning algorithms. *Pure and Applied Geophysics*, *180*, 3477–3494. <https://doi.org/10.1007/s00024-023-03340-9>
- Mohanty, W. K., & Walling, M. Y. (2008). First order seismic microzonation of Haldia, Bengal Basin (India) using a gis platform. *Pure and Applied Geophysics*, *165*, 1325–1350. <https://doi.org/10.1007/s00024-008-0360-6>
- Mukhopadhyay, R., Karisiddaiah, S. M. (2014). The Indian coastline: Processes and landforms. In V. Kale. (Eds.), *Landscapes and Landforms of India*. *World Geomorphological Landscapes*. Springer, Dordrecht. [https://doi.org/10.1007/978-94-017-8029-2\\_8](https://doi.org/10.1007/978-94-017-8029-2_8)
- Mukhopadhyay, A., Hazra, S., Mitra, D., et al. (2016). Characterizing the multi-risk with respect to plausible natural hazards in the Balasore coast, Odisha, India: A multi-criteria analysis (MCA) appraisal. *Natural Hazards*, *80*, 1495–1513. <https://doi.org/10.1007/s11069-015-2035-9>
- Murthy, K. S. R., Subrahmanyam, A. S., Murty, G. P. S., Sarma, K. V. L. N. S., Subrahmanyam, V., Rao, K. M., Rani, P. S., Anuradha, A., Adilakshmi, B. & Devi, T. S. (2006). Factors guiding tsunami surge at the Nagapattinam–Cuddalore shelf, Tamil Nadu, east coast of India. *Current Science*, pp. 1535–1538.
- Murthy, K. S. R., Subrahmanyam, V., Subrahmanyam, A. S., et al. (2010). Land–ocean tectonics (LOTs) and the associated seismic hazard over the Eastern Continental Margin of India (ECMI). *Natural Hazards*, *55*, 167–175. <https://doi.org/10.1007/s11069-010-9523-8>
- Murthy, K. S. R., Subrahmanyam, A. S., & Subrahmanyam, V. (2012). *Tectonics of the eastern continental margin of India*. The Energy and Resources Institute (TERI).
- NASA Shuttle Radar Topography Mission (SRTM)(2013). Shuttle radar topography mission (SRTM) global. Distributed by OpenTopography. <https://doi.org/10.5069/G9445JDF>
- Ngoy, K. I., Qi, F., & Shebitz, D. J. (2021). Analyzing and predicting land use and land cover changes in New Jersey using multi-layer perceptron–Markov chain model. *Earth*, *2*, 845–870. <https://doi.org/10.3390/earth2040050>
- Radhakrishna, B. P. (1989). Suspect tectonostratigraphic terrane elements in the Indian subcontinent. *Journal of Geological Society of India*, *34*, 1–24.
- Rai, A. K., Tripathy, S., & Sahu, S. C. (2015). The May 21st, 2014 Bay of Bengal earthquake: Implications for intra-plate stress regime. *Current Science*, *108*, 9.
- Rai, A. K., Malakar, S., & Goswami, S. (2023). Active source zones and earthquake vulnerability around Sumatra subduction zone. *Journal of Earth System Science*, *132*, 66. <https://doi.org/10.1007/s12040-023-02070-9>
- Rai, A. K., & Nayak, R. K. (2021). Shallow structure and seismic hazard in the Coastal Odisha, India. In: Shandilya, A. K., Singh, V. K., Bhatt, S. C., Dubey, C. S. (eds). *Geological and Geo-Environmental Processes on Earth*. *Springer Natural Hazards*. [https://doi.org/10.1007/978-981-16-4122-0\\_13](https://doi.org/10.1007/978-981-16-4122-0_13)
- Rodcha, R., Tripathi, N. K., & Shrestha, R. P. (2019). Comparison of cash crop suitability assessment using parametric, AHP, and F-AHP methods. *Land*, *8*, 5. <https://doi.org/10.3390/land8050079>
- Saaty, T. L. (1980). *The analytic hierarchy process: Planning, priority setting, resource allocation*. McGraw.
- Salarian, T., Zare, M., Jouri, M. H., Miarrostami, S., & Mahmoudi, M. (2014). Evaluation of shallow landslides hazard using artificial neural network of Multi-Layer Perceptron method in Subalpine Grassland (Case study: Glandrood watershed-Mazandaran). *International Journal of Agriculture and Crop Sciences*, *7*(11), 795–804.
- Satyannarayana, R., Rajesh, B. G. (2021). Seismotectonic map and seismicity parameters for Amaravati area, India. *Arabian Journal of Geosciences* *14*, 2414. <https://doi.org/10.1007/s12517-021-08622-x>
- Singh, S. C., Chauhan, A. P. S., Calvert, A. J., Hananto, N. D., Ghosal, D., Rai, A., & Carton, H. (2012). Seismic evidence of bending and unbending of subducting oceanic crust and the presence of mantle megathrust in the 2004 Great Sumatra earthquake rupture zone. *Earth and Planetary Science Letters*, *321*–322, 166–176. <https://doi.org/10.1016/j.epsl.2012.01.012>
- Sözen, A. (2009). Future projection of the energy dependency of Turkey using artificial neural network. *Energy Policy*, *37*(11), 4827–4833. <https://doi.org/10.1016/j.enpol.2009.06.040>
- Vaz, G. G., Mohapatra, G. P., & Hariprasad, M. (1998). Origin and palaeoenvironmental aspects of red sediment from Bavanapadu-Ichchapuram, Andhra Pradesh. *Journal of Geological Society of India*, *52*, 463–471.
- Worden, C. B., Wald, D. J., Sanborn, J., & Thompson, E. M. (2015). *Development of an open-source hybrid global Vs30 model*. Seismology Society of America.

- Yariyan, P., Zabihi, H., Wolf, I. D., Karami, M., & Amiriyani, S. (2020). Earthquake risk assessment using an integrated fuzzy analytic hierarchy process with artificial neural networks based on GIS: A case study of Sanandaj in Iran. *International Journal of Disaster Risk Reduction*, 50, 101705. <https://doi.org/10.1016/j.ijdrr.2020.101705>
- Yariyan, P., Abbaspour, R. A., Chehreghan, A., Karami, M. R., & Cerdà, A. (2021). GIS-based seismic vulnerability mapping: A comparison of artificial neural networks hybrid models. *Geocarto International*. <https://doi.org/10.1080/10106049.2021.1892208>
- Zhang, G., Eddy Patuwo, B., & Hu, M. Y. (1998). Forecasting with artificial neural networks: The state of the art. *International Journal of Forecasting*, 14, 35–62. [https://doi.org/10.1016/S0169-2070\(97\)00044-7](https://doi.org/10.1016/S0169-2070(97)00044-7)

**Publisher's Note** Springer Nature remains neutral with regard to jurisdictional claims in published maps and institutional affiliations.

Springer Nature or its licensor (e.g. a society or other partner) holds exclusive rights to this article under a publishing agreement with the author(s) or other rightsholder(s); author self-archiving of the accepted manuscript version of this article is solely governed by the terms of such publishing agreement and applicable law.